Austin Journal of Earth Science

Open Access

Austin Publishing Group

Research Article

Idealized Model of Mineral Infillings in Bones of Fossil Freshwater Animals, on the Example of Late Triassic Metoposaurs from Krasiejów (Poland)

Bodzioch A*
Department of Biosystematics, Opole University, Poland
***Corresponding author:** Adam Bodzioch, Department of Biosystematics, Opole University, ul. Oleska 22, 45-052 Opole, Poland

Received: December 12, 2014; **Accepted:** February 24, 2015; **Published:** February 27, 2015

Abstract

Pore spaces preserved in bones are not studied so often, however they contain a very important information about post-mortem history, which is presented below on the example of microscope observations of fossil aquatic amphibians. Cavities from decay of soft tissues have been filled with a few mineral phases, which form more or less complete sequence related to post-mortem events. The most interesting complete sequence is referred to diagenesis of bones buried together with soft parts in fine-grained sediment of a flooding pool. It starts with the surrounding sediment sucked in by outgoing gas bubbles created during bacterial decomposition of soft tissues. Next two generations of infillings (pyrite, substituted in places by siderite, and granular sparite) have been interpreted as a result of sulfate and iron reducing bacteria activity. The two last generations (blocky sparite and barite) have been interpreted as chemical precipitates. Blocky sparite crystallized from pore solution being in equilibrium with respect to carbonates. Barite evidences shift in pore water chemistry (supersaturation with respect to sulfates), according to progressive evaporation of a flooding pool.

Keywords: Metoposaurus; Triassic; Bone; Diagenesis; Taphonomy

Abbreviations

UOBS: Catalogue Acronym of Bones from the "Trias" Documentation Site in Krasiejów, collected at the Opole University in the years 2000-2007; UOPB: Catalogue acronym of bones from the "Trias" Documentation Site in Krasiejów, collected at the Opole University since the year 2008; SEM: Scanning Electron Microscope; EDS: Energy Dispersive Spectroscopy

Introduction

Diagenesis of bones is not an extensively studied topic, apart from remains of selected terrestrial creatures including archaeological materials [1-7] and dinosaurs [8-10]; in addition, alterations of bone tissue are the main topics [1-16]. Rare analysis of infillings of intra-bone spaces are also strongly restricted to archaeological [11] and dinosaurian remains [17,18], while similar studies of other vertebrates are rather unique [19-21]. Thus, an introduction to interpretation of diagenetic events, based on a sequence of mineral phases filling pore spaces in bones of aquatic animals, is the main purpose of this paper.

The study has been carried out on metoposaurs: large, freshwater amphibians living in the Triassic times. Their fossils are best known from Germany [22,23] and Poland [24], where they occur in lacustrine or alluvial plain deposits of the Carnian-Norian age. Paleontological knowledge of those animals is quite broad within the realm of osteology [25,26] and rapidly developing osteohistology [27-32]. Post-mortem history of metoposaurian bones is still unknown apart from the pioneer publication [33], in which the origin of the metoposaur rich bone bed has been explained on the ground of diagenetic studies. Tissue of analysed bones underwent partial dissolution, recrystallization, replacing and cracking, and intra-bone spaces have been completely or nearly completely filled with various mineral phases. Full taphonomic analysis is not yet complete, but simple observations are also valuable for answering certain questions and creation of general hypotheses. Microscope evidence of a sequence of diagenetic events is the first of many necessary steps to be taken in any taphonomic analysis of bones, however only this step is described below. A complete sequence of infillings is referred to biogeochemically induced diagenesis of bones, which have been buried together with soft tissues.

Materials and Methods

The studied material has been collected from the lower bone horizon of the "Trias" Documentation Site in Krasiejów [24,33,34], during excavation field works organized and conducted by the Laboratory of Paleobiology of the Opole University since the year 2000. Bones occur in about 0,8 m thick, grey to red unstructured clay/mud layer, only slightly lithified, which is underlain by red paleosoil and covered in places by thin (0-10 cm), discontinuous limestone of pedogenic origin. The sediment consists of clay minerals (illite, smectite, chlorite and palygorskite), subordinate grains of quartz, muscovite, feldspar, and some heavy minerals [35]. General sedimentologic and diagenetic characteristics show that the bone bed has been deposited as a mud flow [36] in an ephemeral flooding pool [33].

A skull, lower jaw, clavicle, interclavicle, 2 ribs, 8 long bones and 20 vertebral intercenters of metoposaurs were selected to make 76 thin sections (for both osteohistological and diagenetic purposes), which have been prepared at the Institute of Geology of the A. Mickiewicz

Citation: Bodzioch A. Idealized Model of Mineral Infillings in Bones of Fossil Freshwater Animals, on the Example of Late Triassic Metoposaurs from Krasiejów (Poland). Austin J Earth Sci. 2015;2(1): 1008.

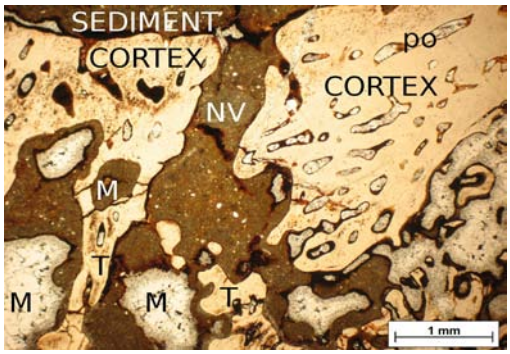

Figure 1: General osteohistological and diagenetic features of vertebral intercenters (UOPB1003, thin section, plane polarized light). The sediment fills a main nutrition vessel (NV) going through the cortex to inner part of the vertebrae. Medullary cavities (M) are filled with sediment (white M), sediment and then calcite (black M), or with sediment, then pyrite (now weathered, black areas) and then calcite (bottom-right part of the photo). T: trabeculae that form spongy bone. Within the cortex, primary osteons are visible as oval structures (po). They are filled with the sediment (if connecting surface of the cortex), pyrite (black) and calcite (light colored areas).

Figure 2: Sediment padding (S) in spongy bone of the vertebral intercentrum UOPB 1009 (thin section, cross polarized light), followed by pyrite (black lines) and calcite (C). Densely packed pyrite framboids are visible in the rectangle.

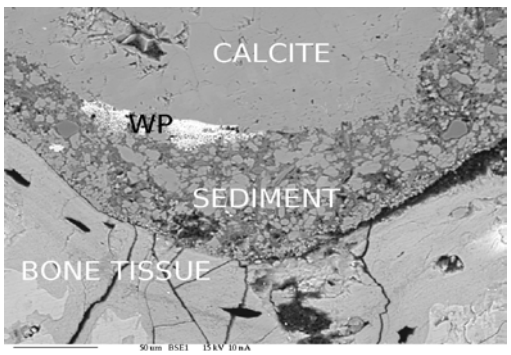

Figure 3: The same as in Figure 2, SEM image. Weathered pyrite (WP) is visible as white areas between the sediment and calcite.

University in Poznań (Poland) and at the Steinmann Institute für Paläontologie (Bonn University, Germany). The thin sections were examined with a standard petrographic microscope (Olympus Provis AX70) equipped with a digital camera. Simple SEM and EDS analyses have been additionally done to verify petrographic identification of mineral phases using Hitachi S-3700N apparatus.

Results and Discussion

Primary pore spaces inside studied bones include medullary cavities, erosional rooms, components of the vascular system (nutrition vessels, primary and secondary osteons), and osteocyte lacunae together with Volkmann canals. Mineral infillings consist of surrounding sediment, pyrite, siderite, calcite and barite, however, the amount of particular type of infilling may vary in wide ranges among the bones. Only calcite occurs in every bone, and sometimes is the only mineral phase. In other bones, calcite is accompanied by one or more minerals. Sometimes, mineral infillings form a sequence, which is best developed in large medullary cavities and erosional rooms, starting from sediment and following by pyrite, siderite and calcite, and ending with barite. At the same time, small pore spaces in compact bone are usually filled with single mineral phase (pyrite or calcite) or with a pyrite-calcite association. Variation in the development of mineral infillings results from secondary deposition of bones coming from various primary diagenetic environments, and from different post-mortem history of particular specimens and their bones. The complete sequence refers to bones, which have been interpreted as buried together with soft tissues.

The complete sequence starts with surrounding sediment, which fills large vessels going through the cortex to internal cavities (Figure 1) and, in the cavities, it forms a thin, nearly isopachous padding around their surface (Figure 2). In all cases of infillings, sediment is cemented by calcium carbonate and, inside the cavities, additionally by pyrite.

Two modes of infiltration of sediment into bone interior can be discussed: hydrodynamic washing in, or sucking in by vacuum created by outgoing gas bubbles originated during decomposition of soft tissues. In the first case, the sediment must be deposited gravitationally at the bottom surface of cavities; isopachous forms of sediment envelopes may have arisen as a result of rolling bones along the bottom, which was impossible because of quiet water environment [34]. Therefore, vacuum seems to be the only force counteracting gravity that allowed clay particles to adhere uniformly to the entire surface of cavities.

Pyrite makes the second generation of infillings, where sediment is present, or the first generation in other cases of its occurrence. Apart from admixture in sediment infillings, it occurs as (1) more or less continuous cover on sediment envelopes (Figure 2,3) or bone tissue (where sediment is absent), separating them from next generation calcite (Figure 4), as (2) inclusions of framboidal forms in the calcite cement (Figure 5), or as (3) mineral filling small pores within the cortex (Figure 6,7). In the last case, pyrite can be associated by calcite.

Framboidal shape of pyrite can be interpreted as a result of bacterially induced precipitation of iron sulfide in anoxic environment, which is widely known since Berner's studies [37,38] and commonly accepted [39-44]. In this case, bacterial interpretation is supported by co-occurrence of pyrite and calcite (metabolism of sulfate reducing bacteria releases hydrogen ions, which destruct calcium carbonates and phosphates, and then concentration of both calcium and bicarbonate ions increases up to oversaturation of pore water with respect to calcium carbonate, and finally, to secondary

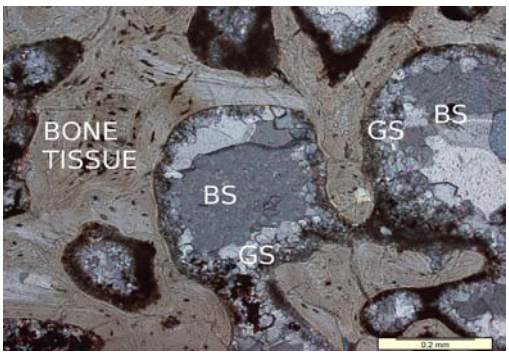

Figure 4: Pyrite covering directly bone tissue (black areas), and followed by two calcite generations: granular (GS) and blocky sparite (BS). Thin section, plane polarized light, vertebral intercentrum UOPB1009.

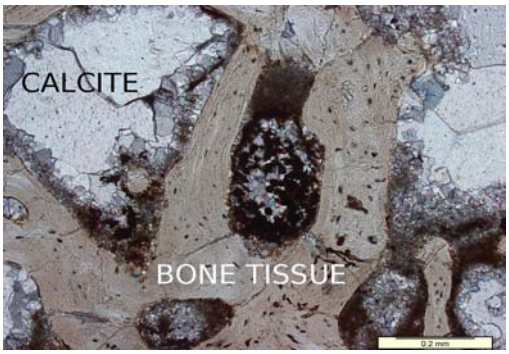

Figure 5: Framboidal pyrite floating in granular sparite (best visible in the center). Thin section, plane polarized light, vertebral intercentrum UOPB1009.

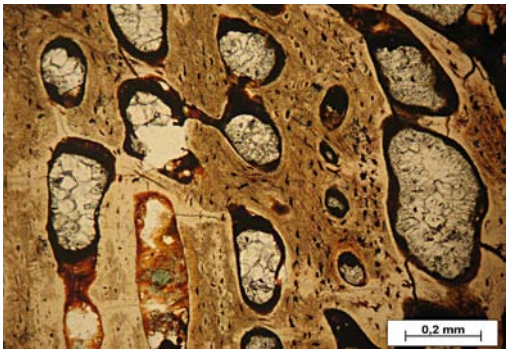

Figure 6: Pyrite (black) and calcite (light-grey) filled primary osteons in the cortex. Thin section, ordinary light, vertebral intercentrum UOPB1003.

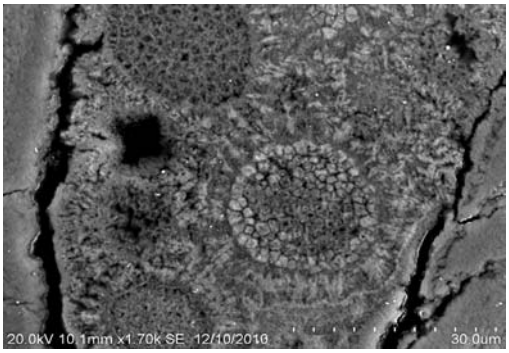

Figure 7: Framboidal pyrite in a primary osteon within the cortex. SEM image, vertebral intercentrum UOPB1009.

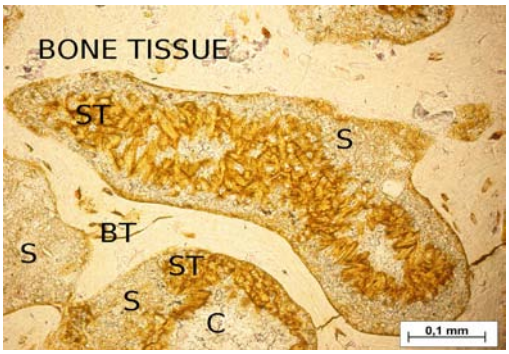

Figure 8: Siderite crystals (ST) encrusting the sediment (S) or bone tissue (BT), and followed by calcite (C). Thin section, ordinary light, vertebral intercentrum UOPB1007.

precipitation of calcite) [45]. Pyrite framboids floating in calcite crystals suggest simultaneous precipitation of the two minerals, and then, fast evolving pore-fluids chemistry (vanishing of sulfides and development of carbonate-dominated water).

Siderite occurs in external parts of spongy bone instead of pyrite, i.e. it covers either sediment padding or bone tissue (Figure 8). Additionally, siderite forms incrustations on the outer surface of some bones.

Sedimentary siderite is known as mineral formed under dysoxic conditions [46-49], whereby its precipitation is mediated by sulfate and iron reducing bacteria most often [48-52]. Therefore, the position of siderite in external part of spongy bone (while the internal part is occupied by pyrite) suggest centimeter-scale gradient in oxygenation of the bone interior, and the occurrence of pyrite in primary osteons of the cortex shows even less, millimeter-scale gradient throughout bones. Such precision in oxygenation gradient is typical for bacterial decomposition of soft tissue within highly restricted microenvironments, where ions exchange between the microenvironment of soft tissue decay and surrounding fluids is strongly limited. Of course, bone tissue itself and sediment, clogging main nutrition vessels, were natural barriers for migration of ions.

Calcite is the main mineral in pore spaces, occurring commonly in both spongy and compact bone, and is represented by at least three generations: micrite cementing sediment envelopes, granular, inclusion-rich sparite cement (older generation), and blocky sparite cement (younger generation). In spongy bone, both types of sparite can cover pyrite lamina (Figure 2), siderite encrustation (Figure 8), or bone tissue (Figure 4,5). Independently, sparite cement fills also primary osteons in the cortex (Figure 7). The boundary between the two generations of sparite cement is usually sharp, which speaks for rapid change in pore water chemistry and rate of crystallisation. Granular sparite can be referred to relatively fast growth of evenly dispersed crystals, i.e. to high supply of both calcium (with other accompanying divalent cations) and bicarbonate ions, while blocky sparite to slow, steady growth, when supply of ions was low, i.e. in the conditions of chemical equilibrium [53-55]. Change in the mode of crystallization could be caused by termination of bacterial activity, which, in turn, could be a result of complete decay of soft tissues

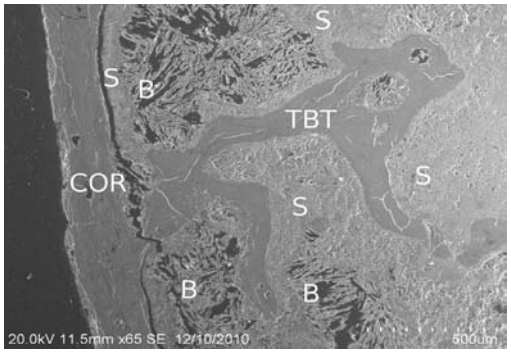

Figure 9: Barite crystals (B) in a rib UOPB1021, SEM image. S: sediment, BS: blocky sparite , COR: cortex, TBT: trabecular bone tissue.

within the bones. That conclusion supports also framboidal pyrite floating in calcite crystals (Figure 4), indicating rapidly decreasing supply of hydrosulfide ions when sparite crystallization began. Thus, we can speak about early diagenesis related to the short time of bacterial activity, and late diagenesis related to chemical precipitation of mineral phases.

Barite is the last generation of infillings, which occurs in small amounts within the largest cavities of spongy bone (Figure 9). Its occurrence speaks clearly for radical change in pore water chemistry from supersaturation with respect to carbonates, to supersaturation with respect to sulfates. According to interpreted depositional history [33] and data about recent environments [6] that shift in water chemistry can be explained as a result of progressive evaporation of a flooding pool, in which the bones had been buried.

Conclusion

Described bones have been buried in a flooding pool, within fine-grained sediment, as parts of buried alive animals. The bones were successively filled with the surrounding sediment, pyrite substituted in places by siderite, granular sparite, blocky sparite and barite (Figure 10). Sediment was sucked in by outgoing gas bubbles originated during bacterial decomposition of soft tissues. Bacterial sulfate reduction led subsequently to crystallization of pyrite and granular sparite, and it ended together with the beginning of crystallization of blocky sparite. At the same time, in the outer part of spongy bone, siderite was forming according to activity of iron reducing bacteria. Next generations of infillings were formed from pore waters evolved according to evaporation of the flooding pool. Blocky sparite crystallized first, as long as supply of both calcium and bicarbonate ions existed. Barite crystallized later, after supersaturation of pore waters by sulfates, according to progressive evaporation. Therefore, early diagenesis is represented by biogeochemical, while late diagenesis by chemical precipitation of mineral phases.

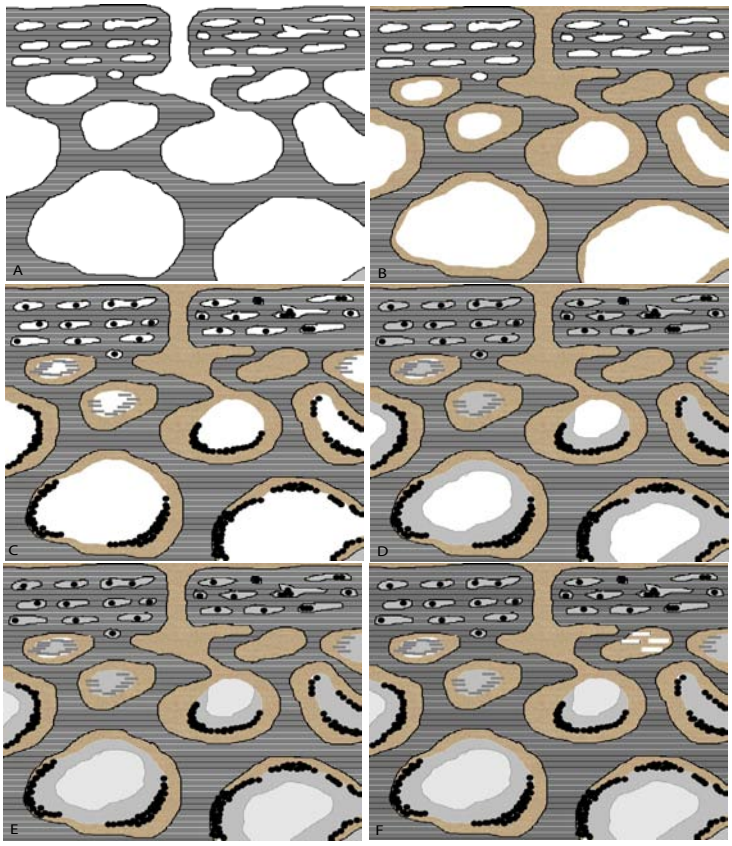

Figure 10: Idealized sequence of infillings in bones buried together with soft tissue in fine grained sediment, at the bottom of a freshwater reservoir. **A**) Bone with intra-skeletal pores partly occupied by soft tissue (white). **B)** Sediment infill. **C)** Pyrite (black) and siderite (grey laths) crystallization, and cementation of sediment envelopes by pyrite and micrite. **D)** Precipitation of granular sparite. The end of bacterial influence on infillings. **E)** Precipitation of blocky sparite. **F)** Precipitation of barite (white laths).

Of course, all the above interpretations need a high precision geochemical evaluation of their accuracy. However, it is clearly visible that microscope analysis of mineral infillings in pore spaces gives a very good conceptual framework to exact studies and further explanations.

References

1. Smith CI, Nielsen-Marsh CM, Jans MME, Collins MJ. Bone diagenesis in the European Holocene I: patterns and mechanisms. J Archaeol Sci. 2007; 34: 1485-1493.
2. Turner-Walker G, Jans M. Reconstructing taphonomic histories using histological analysis. Palaeogeogr Palaeoclim Palaeoecol. 2008; 266: 227-235.
3. Tütken T, Vennemann TW, Pretzschner HU. Early diagenesis of bone and tooth apatite in fluvial and marine settings: Constraints from combined oxygen isotope, nitrogen and REE analysis. Palaeogeogr Palaeoclim Palaeoecol. 2008; 266: 254-268.
4. Tütken T, Vennemann T, editors. Fossil bones and teeth: preservation or alteration of biogenic compositions? Palaeogeogr Palaeoclim Palaeoecol. 2011; 310: 1-8.
5. Balter V, Zazzo A, editors. Bone and enamel diagenesis: From the crystal to the environment – A tribute to Jean Fran?ois Saliège. Palaeogeogr Palaeoclim Palaeoecol. 2014; 416.
6. Maurer A-F, Person A, Tütken T, Amblard-Pison S, Ségalen L. Bone diagenesis in arid environment: An intra-skeletal approach. Palaeogeogr Palaeoclim Palaeoecol. 2014; 416: 17-29.
7. Gutierez MA. Bone Diagenesis and Taphonomic History of the Paso Otero 1 Bone Bed, Pampas of Argentina. J Archaeol Sci. 2001; 28: 1277-1290.
8. Kolodny Y, Luz B, Sander M, Clemens WA. Dinosaur bones: fossils or pseudomorphs? The pitfalls of physiology reconstruction from apatitic fossils. Palaeogeogr Palaeoclim Palaeoecol. 1996; 126: 161-171.
9. Elorza J, Astibia H, Murelaga X, Pereda-Suberbiola X. Francolite as a diagenetic mineral in dinosaur and other Upper Cretaceous reptile bones: microstructural, petrological and geochemical features. Cretaceous Res. 1999; 20: 169-187.
10. Goodwin MB, Grant PG, Bench G, Holroyd PA. Elemental composition and diagenetic alteration of dinosaur bone: Distinguishing micro-scale spatial and compositional heterogeneity PIXE. Palaeogeogr Palaeoclim Palaeoecol. 2007; 253: 458-476.
11. Trueman CNG, Behrensmeyer AK, Tuross N, Weiner S. Mineralogical and compositional changes in bones exposed on soil surfaces in Amboseli National Park, Kenya: diagenetic mechanisms and the role of sediment pore fluids. J Archaeol Sci. 2004; 31: 721-739.
12. Sasso GD, Maritan L, Usai D, Angelini I, Artioli G. Bone diagenesis at the micro-scale: Bone alteration patterns during multiple burial phases at Al Khiday between the Early Holocene and the II century AD. Palaeogeogr Palaeoclim Palaeoecol. 2014; 416: 30-42.
13. Hubert JF, Panish PT, Chure DJ, Prostak KS. Chemistry, microstructure, petrology, and diagenetic model of Jurassic dinosaur bones, Dinosaur National Monument, Utah. J Sed Res. 1996; 66: 531-547.
14. Pfretzschner HU, Tütken T. Rolling bones – Taphonomy of Jurassic dinosaur bones inferred from diagenetic microcracks and mineral infillings. Palaeogeogr Palaeoclim Palaeoecol. 2011; 310: 117-123.
15. Dumont M, Kostka A. Sander PM, Borbely A, Kaysser-Pyzalla A. Size and size distribution of apatite crystals in sauropod fossil bones. Palaeogeogr Palaeoclim Palaeoecol. 2011; 310: 108-116.
16. Suarez CA, Macpherson GL, González LA, Grandstaff DE. Heterogeneous rare earth element (REE) patterns and concentrations in a fossil bone: Implications for the use of REE in vertebrate taphonomy and fossilization history. Geochimica et Cosmochimica Acta. 2010; 74: 2970-2986.
17. Piga G, Brunetti A, Lasio B, Malfatti L, Galobart À, Vecchia FMD, et al. New insights about the presence of celestite into fossil bones from Molí del Baró 1 site. Appl. Phys. 2014.
18. Bauluz B, Gasca JM, Moreno-Azanza M, Canudo JI. Unusual replacement of biogenic apatite by aluminum phosphate phases in dinosaur teeth from the Early Cretaceous of Spain. Lethaia. 2014.
19. Reichel M, Schulz CL, Pereira VP. Diagenetic pattern of vertebrate fossils from the traversodontidae biozone, Santa Maria Formation (Triassic), southern Brazil. Rev Brazil Paleont. 2005; 8: 173-180.
20. Piga G, Santos-Cubedo A, Solà SM, Brunetti A, Malgosa A, Enzo S. An X-ray Diffraction (XRD) and X-ray Fluorescence (XRF) investigation in human and animal fossil bones from Holocene to Middle Triassic. J Archaeol Sci. 2009; 36: 1857-1868.
21. Wings O. Authigenic minerals in fossil bones from the Mesozoic of England: poor correlation with depositional environments. Palaeogeogr Palaeoclim Palaeoecol. 2004; 204: 15-32.
22. Fraas E. Labyrinthodonten der Schwäbischen Trias. Palaeontographica. 1889; 36: 1-158.
23. Milner AR, Schoch RR. The latest metoposaurids from Europe. N Jahrbuch für Geol Paläont Abh. 2004; 232: 231-252.
24. Dzik J, Sulej T. A review of the early Late Triasssic Krasiejów biota from Silesia, Poland. Palaeont Polon. 2007; 64: 3-27.
25. Sulej T. Species discrimination of the Late Triassic temnospondyl amphibian Metoposaurus diagnosticus. Acta Palaeont Polon. 2002; 47: 535-546.
26. Sulej T. Osteology, variability, and evolution of Metoposaurus, a temnospondyl from the Late Triassic of Poland. Palaeont Polon. 2007; 64: 29-139.
27. Gądek K. Palaeohistology of ribs and clavicle of Metoposaurus diagnosticus from Krasiejów (Upper Silesia, Poland). Opole Sci Soc Nature J. 2012; 45: 39-42.
28. Gruntmejer K. Morphology and function of cranial sutures of the Late Triassic amphibian Metoposaurus diagnosticus (Temnospondyli) from southwest Poland. Jagt-Yazykova E, Jagt JWM, Bodzioch A, Konietzko-Meier D, editors. In: Krasiejów – palaeontological inspirations. ZPW Plik Bytom. 2012; 36-56.
29. Konietzko-Meier D, Klein N. Unique growth pattern of Metoposaurus diagnosticus krasiejowensis (Amphibia, Temnospondyli) from the Upper Triassic of Krasiejów, Poland. Palaeogeogr Palaeoclim Palaeoecol. 2013; 370: 145-157.
30. Konietzko-Meier D, Sander PM. Long bone histology of Metoposaurus diagnosticus (Temnospondyli) from the Late Triassic of Krasiejów (Poland) and its paleobiological implications. J V P. 2013; 33: 1003-1018.
31. Konietzko-Meier D, Bodzioch A, Sander PM. Histological characteristics of the vertebral intercentra of Metoposaurus diagnosticus (Temnospondyli) from the Upper Triassic of Krasiejów (Upper Silesia, Poland). EESTRSE. 2013; 103: 237-250.
32. Konietzko-Meier D, Danto M, Gądek K. The microstructural variability of the intercentra among temnospondyl amphibians. Biol J Linnean Soc. 2014; 112: 747-764.
33. Bodzioch A, Kowal-Linka M. Unravelling the origin of the Late Triassic multitaxic bone accumulation at Krasiejów (S Poland) by diagenetic analysis. Palaeogeogr Palaeoclim Palaeoecol. 2012; 346-347: 25-36.
34. Gruszka B, Zieliński T. Evidence for a very low-energy fluvial system: a case study from the dinosaur-bearing Upper Triassic rocks of Southern Poland. Geol Quart. 2008; 52: 239-252.
35. Zatoń M, Piechota A, Stankiewicz E. Late Triassic charophytes around the bone-bearing bed in Krasiejów (SW Poland) – palaeoecological and environmental remarks. Acta Geol Polon. 2005; 55: 283-293.
36. Szulc J. Sedimentary environments of the vertebrate-bearing Norian deposits from Krasiejów, Upper Silesia (Poland). Hallesches Jahrbuch für Geowiss Reiche B. 2005; 19: 161-170.
37. Berner RA. Sedimentary pyrite formation. Amer J Sci. 1970; 268: 1-23.

38. Berner RA. Sedimentary pyrite formation: an update. Geochimica et Cosmochimica Acta. 1984; 48: 605-615.

39. Kohn MJ, Riciputi LR, Stakes D, Orange DL. Sulfur isotope variability in biogenic pyrite: Reflections of heterogeneous bacterial colonization? Amer Mineral. 1998; 83: 1454-1468.

40. Roychoudhury AN, Kostka JE, van Cappellen P. Pyritization: a palaeoenvironmental and redox proxy reevaluated. Estuarine Coastal and Shelf Science. 2003; 57: 1183-1193.

41. Szczepanik P, Sawłowicz Z, Bąk M. Pyrite framboids in pyritized radiolarian skeletons (Mid-Cretaceous of the Pieniny Klippen Belt, Western Carpathians, Poland). Ann Soc Geol Polon. 2004; 74: 35-41.

42. Folk JR. Nannobacteria and the formation of framboidal pyrite: Textural evidence. J Earth System Sci. 2005; 114: 369-374.

43. MacLean LC, Tyliszczak T, Gilbert PU, Zhou D, Pray TJ, Onstott TC, et al. A high-resolution chemical and structural study of framboidal pyrite formed within a low-temperature bacterial biofilm. Geobiology. 2008; 6: 471-480.

44. Yiming G, Shi GR, Weldon EA, Bin H, Yongan Q, Guoheng Z. Pyrite Framboids Showing Pseudomorphisms of Microbial Colonies within the Permian Zoophycos Spreiten from Southeastern Australia. J Earth Sci. 2009; 21: 381-382.

45. Bodzioch A. Biogeochemical diagenesis of the Lower Muschelkalk of Opole region. Poznan: Wydawnictwa Naukowe UAM. 2005.

46. Lim DI, Jung HS, Yang SY, Yoo HS. Sequential growth of early diagenetic freshwater siderites in the Holocene coastal deposits, Korea. Sedimentary Geology. 2004; 169: 107-120.

47. Driese SG, Ludvigson GA, Roberts JA, Fowle DA, Gonzàles LA, Smith JJ, et al. Micromorphology and stable isotope geochemistry of historical pedogenic siderite forming in pah-contaminated alluvial clay soils, Tennessee, U.S.A. J Sed Res. 2010; 80: 943-954.

48. Sánchez-Róman M, Fernández-Remolar D, Amils R, Sánchez-Navas A, Schmid T, Martin-Uriz PS, et al. Microbial mediated formation of Fe-carbonate minerals under extreme acidic conditions. Nature Scientific Reports 2014; 4, 4767.

49. Roh Y, Zhang CL, Vali H, Lauf RJ, Zhou J, Phelps TJ. Biogeochemical and environmental factors in Fe biomineralization: magnetite and siderite formation. Caly and Clays Minerals. 2003; 51: 83-95.

50. Pye K, Dickson JA, Schiavon N, Coleman ML, Cox M. Formation of siderite-Mn-calcite-iron sulphide concretions in intertidal marsh and sandflat sediments, North Nofolk, England. Sedimentology. 1990; 37: 325-343.

51. Lovley DR. Microbial Fe(III) reduction in subsurface environments. FEMS Microbiol. Rev. 1997; 20: 305-313.

52. Tobias C, Neubauer SC. Salt Marsh Biogeochemistry – An Overview. Perillo GME, Volanski E, Cahoon DR, Brinson MM, editors. In: Coastal Wetlands an Integrated Approach. Elsevier. 2009; 445-492.

53. Folk RL, Land LS. Mg/Ca ratio and salinity: two controls over crystallization of dolomite. AAPG Bull. 1975; 59: 60–68.

54. Teng HH, Dove PM, Joreo JJde. Kinetics of calcite growth: Surface processes and relationships to macroscopic rate laws. Geochimica et Cosmochimica Acta. 2000; 64: 2255-2266.

55. Yoreo JJde, Vekilov PG. Principles of Crystal Nucleation and Growth. Dove PM, Yoreo JJde, Weiner S, editors. In: Biomineralization. Mineralogical Society of America. 2003; 54: 57-94.

Austin J Earth Sci - Volume 2 Issue 1 - 2015
ISSN : 2380-0771 | www.austinpublishinggroup.com

Citation: Bodzioch A. Idealized Model of Mineral Infillings in Bones of Fossil Freshwater Animals, on the Example of Late Triassic Metoposaurs from Krasiejów (Poland). Austin J Earth Sci. 2015;2(1): 1008.